Published in final edited form as:
J Cell Physiol. 2009 June ; 219(3): 563–571. doi:10.1002/jcp.21701.

Secretome From Mesenchymal Stem Cells Induces Angiogenesis Via Cyr61

ROSENDO ESTRADA[1], **NA LI**[1], **HARSHINI SAROJINI**[1], **JIN AN**[1], **MENQ-JER LEE**[1,2], and **EUGENIA WANG**[1,3,*]

[1]Gheens Center on Aging, University of Louisville School of Medicine, Louisville, Kentucky

[2]Department of Microbiology and Immunology, University of Louisville School of Medicine, Louisville, Kentucky

[3]Department of Biochemistry and Molecular Biology, University of Louisville School of Medicine, Louisville, Kentucky

Abstract

It is well known that bone marrow-derived mesenchymal stem cells (MSCs) are involved in wound healing and regeneration responses. In this study, we globally profiled the proteome of MSCs to investigate critical factor(s) that may promote wound healing. Cysteine-rich protein 61 (Cyr61) was found to be abundantly present in MSCs. The presence of Cyr61 was confirmed by immunofluorescence staining and immunoblot analysis. Moreover, we showed that Cyr61 is present in the culture medium (secretome) of MSCs. The secretome of MSCs stimulates angiogenic response in vitro, and neovascularization in vivo. Depletion of Cyr61 completely abrogates the angiogenic-inducing capability of the MSC secretome. Importantly, addition of recombinant Cyr61 polypeptides restores the angiogenic activity of Cyr61-depleted secretome. Collectively, these data demonstrate that Cyr61 polypeptide in MSC secretome contributes to the angiogenesis-promoting activity, a key event needed for regeneration and repair of injured tissues.

Wound healing in adults depends on the presence of functional stem cells capable of replicating and differentiating into other type of cells. Bone marrow-derived mesenchymal stem cells (MSCs) are known for their ability to differentiate into other cell types, such as bone, cartilage, muscle, adipocytes, stromal cells, as well as fibroblasts (Prockop, 1997; Weissman, 2000; Phinney and Prockop, 2007). It has been also demonstrated that MSCs can differentiate into endothelial cells, suggesting the potential of MSCs in neovascularization (Tomanek and Schatteman, 2000). In addition, the possible involvement of human bone-marrow-derived stem cells in neovacularization was proposed, based on the fact that these cells are able to contribute to tumor angiogenesis in vivo (Reyes et al., 2002). Furthermore, accumulating evidence suggests that bone marrow-derived MSCs may promote tissue repair by secreting factors which are able to recruit various types of cells critical for regeneration of injured tissue (Chamberlain et al., 2007; Phinney and Prockop, 2007).

Therefore, investigating the proteins secreted by MSCs is essential to understand the molecular mechanisms by which MSCs regulate wound healing and regeneration processes. Indeed, Sze et al. (2007) have assessed the secretion proteome of human embryonic stem

*Correspondence to: Eugenia Wang, School of Medicine, University of Louisville, 580 S. Preston St., Louisville, KY 40202. e0wang01@gwise.louisville.edu.

Additional Supporting Information may be found in the online version of this article.

cells (hESC)-derived MSCs by LC-MS/MS and antibody array to identify paracrine factors that may have therapeutic effect. In that study, they found a number of MSC secreted products that may have functional implications in modulating injury repairing processes. In addition, the transcriptome analysis of human and murine MSCs has also identified a variety of regulatory proteins that function in angiogenesis, hematopoiesis, neural activities, immunity and defense (Phinney, 2007).

In the present study, we investigate possible factor(s) synthesized by MSCs that may be functionally important in tissue regeneration. We used high-resolution, two-dimensional liquid chromatography tandem mass spectrometry (LC-MS/MS) to globally profile the proteome of murine MSCs (mMSCs). We found Cyr61 (also known as CCN1), a member of the CCN family of polypeptides, to be expressed in mMSCs. The presence of this protein in MSCs was confirmed by immunoblot and immunohistochemical analysis. In addition, Cyr61 polypeptides are observed in the secretome of MSCs. Moreover, the MSC secretome induces morphogenesis of endothelial cells in vitro, and neovascularization in vivo. Utilizing the immunodepletion and reconstitution procedure on the secretome, we demonstrated that Cyr61 is a key factor in MSC secretome which contributes to the angiogenic response.

Experimental Procedures

Reagents

Horseradish peroxidase (HRP)-conjugated goat anti-rabbit immunoglobin (IgG) was obtained from MP Biomedicals (Solon, OH), rabbit polyclonal anti-Cyr61 from Santa Cruz Biotechnology (Santa Cruz, CA), matrigel from BD Biosciences (San Jose, CA), amine-reactive isobaric tagging reagents (iTRAQ) from Applied Biosystems (St. Louis, MO), and penicillin-streptomycin from Mediatech, Inc. (Herndon, VA). Human recombinant cysteine-rich protein 61 (Cyr61) was obtained from Cell Sciences (Canton, MA). Trypan Blue stain solution (0.4%) from Cellgro (Lawrence, KS).

Animals

Athymic mice were obtained from Charles River Laboratories (Wilmington, MA), and C57/B6 male mice from the Jackson Laboratories (Bar Harbor, ME). All animal protocols were reviewed and approved by the Institutional Animal Care and Use Committee of the University of Louisville according to National Institutes of Health guidelines for animal research.

Cell culture

Human umbilical vein endothelial cells (HUVECs) and human pulmonary artery endothelial cells (HPAECs) were obtained from Clonetics (Lonza BioScience, Walkersville, MD). Cells were cultured in M199 medium supplemented with 10% (v/v) heat-inactivated fetal bovine serum (Hyclone, Logan, UT), heparin-stabilized endothelial cell growth factors and antibiotics (Hla and Maciag, 1990; Lee et al., 1999). Murine mesenchymal stem cells were obtained from tibias and femurs of 28- to 29-month-old C57/B6 male mice, as we described previously (Sarojini et al., 2008). Briefly, bone marrow cells were flushed from tibias and femurs with Dulbecco minimal essential medium (DMEM) containing penicillin/streptomycin antibiotics. The cells were dispersed with the use of a pipette to obtain single cell suspension, and transferred into a culture dish with 10% (v/v) fetal bovine serum (FBS) in DMEM medium and antibiotics. The cells were maintained at 37°C in a humidified 5% CO_2 incubator. After 72 h, media containing non-adherent cells were removed. Subsequently, single cell clones were obtained by serial dilution. Characterization of these cells was performed by flowcytometric analysis of the expression of marker proteins for stem cells as we recently reported (Sarojini et al., 2008).

Liquid chromatography tandem mass spectrometry (LC-MS/MS)

For profiling cellular proteome, cells were collected in phosphate buffered saline (PBS) by cell scraper. After centrifugation (500*g*, 5 min) at 4°C, cell pellets were resuspended in 0.5 M triethylammonium bicarbonate buffer (TEAB) (Sigma–Aldrich, St. Louis, MO) containing protease inhibitor cocktail (Roche Applied Science, Indianapolis, IN). Cell extracts were obtained by constant agitation at 4°C for 30 min, followed by sonication in an ultrasonic bath (FS6, Fisher Scientific, Philadelphia, PA) for 5 min at 4°C. After centrifugation (13,000*g*) for 30 min at 4°C, protein concentration was determined by Bradford protein assay reagent (Bio-Rad, Hercules, CA). Proteins were then digested with trypsin. The resulting tryptic peptides were resolved by high performance liquid chromatography (HPLC), and analyzed by the QSTAR XL hybrid LC-MS/MS, essentially as we described (Cong et al., 2006; Sarojini et al., 2008).

Data processing

ProteinPilot™ 2.0.1 software (Applied Biosystems, revision number: 67476) with the Paragon Algorithm was used for the identification of proteins. This software allows to distinguish protein isoforms, and suppress false positives using the embedded industry-leading Pro Group™ Algorithm for protein grouping analysis. Tandem mass spectrometry data were searched against the NCBI mouse protein database. The parameters used for searching were 95% confidence (unused ProtScore > 1.30) for protein identification threshold, trypsin as enzyme, methylmethanethiosulfonate-labeled cysteine as fixed modification, biological modification and amino acid substitution as ID focus and thorough mode as search method. Three thousand eight hundred and thirty spectra were identified and two thousand and fifty six peptides were found.

Conditioned medium of mesenchymal stem cell (MSC) cultures

MSCs were grown to 90–100% confluency in 100 mm Petri dishes (Falcon, BD Biosciences, San Jose, CA). Cells were washed four times with serum-free media (plain DMEM), and incubated with 5 ml of plain DMEM at 37°C in a humidified 5% (v/v) CO_2 incubator for 24 h. The medium containing secreted proteins was collected, centrifuged (1000*g*, 10 min) at 4°C, and filtered with a 0.22-μm low protein binding membrane (Millipore, Bedford, MA). Protein concentration was determined by Bradford protein assay (Bio-Rad). The collected medium with secreted proteins was concentrated by ultrafiltration in a positive-pressure ultrafiltration module (Amicon, Millipore, Billerica, MA) fitted with a 10-kDa MWCO membrane (Millipore). The concentrated media (designated as the MSC secretome) were stored at −80°C for future analysis.

Immunoblotting analysis

Equal amounts of proteins from secretome and cell extracts were separated on 9% (v/v) SDS–PAGE gels, and transferred to nitrocellulose membranes (Schleicher and Schuell, Whatman, Florham Park, NJ). Membranes were blocked with 5% (w/v) non-fat dry milk (LabScientific, Livingston, NJ). After washing, membranes were incubated with individual primary antibodies (1:1,000 dilution) on a rocking shaker at 4°C overnight. Membranes were washed and incubated with HRP-conjugated second antibody (1:1,000 dilution) for 1 h at room temperature, followed by incubation with chemiluminescence reagents (Pierce, Rockford, IL) for 1 min. Protein bands were detected by exposure to autoradiography film (Labscientific).

Immuno-depletion of Cyr61

Protein A/G agarose beads (Pierce) were cross-linked with anti-Cyr61 immunoglobulin (IgG), as previously described (Lee et al., 1999). Beads cross-linked with purified normal

rabbit IgG were used as a negative control. MSC secretome was incubated with anti-Cyr61 or control IgG beads at room temperature for 1 h. Subsequently, the beads and supernatant fractions were separated by centrifugation at 1,000*g* for 1 min. The efficacy of Cyr61depletion was confirmed by immunoblot analysis with anti-Cyr61 antibody.

Immunofluorescence analysis

Mesenchymal stem cells (MSCs) were plated in 35 mm glass-bottom dishes (MatTek Corporation, MA). After 48 h, cells were fixed with 4% (w/v) paraformaldehyde, and permeabilized with 0.25% (w/v) Triton-X in PBS. Rabbit anti-Cyr61 antibody (1:200 dilution) was used for Cyr61 staining, followed by Alexa568-conjugated goat anti-rabbit antibody (1:400 dilution), (Molecular Probes, Invitrogen, Carlsbad, CA). The immunofluorescence staining was analyzed by an Olympus Fluoview FV1000 confocal microscope (Olympus, Center Valley, PA) or Axiovert 200 M epi-fluorescence microscope (Carl Zeiss, Thornwood, NY).

Capillary morphogenesis assay

Matrigel (BD Bioscience, 10 mg protein/ml) was added into 24-well tissue culture plates, and polymerized for 1 h at 37°C. HUVECs were trypsinized, resuspended in DMEM, plated (5×10^4 cells) onto matrigel, and incubated at 37°C. After 18 h, cells in five replicate fields of triplicate wells were digitally photographed with an Axiovert 200 M epi-fluorescence microscope (Carl Zeiss). Total tubular length was quantified by image analysis software (Axio Vision, Carl Zeiss). The total tubular length was calculated as average of the total tubule length from three wells, five random fields per well.

In vivo angiogenic assay

In vivo angiogenic assay using the matrigel implant method in athymic mice was performed as we previously described (Lee et al., 1999). Briefly, athymic mice were injected subcutaneously with 1 ml of matrigel containing the indicated amounts of proteins from MSC secretome. After 12 days, mice were sacrificed. Matrigel implants were recovered along with underlying skin, fixed with 4% (w/v) formaldehyde and were photographed under a dissecting microscope (SZX16, Olympus). Subsequently, matrigel plugs were embedded in Tissue-Tek with optimal cutting temperature (OCT) compound (Sakura Finetek, Torrance, CA) and frozen at 80°C. The matrigel plugs were cryostat sectioned (8 μm) and stained with hematoxylin/eosin reagents. Each treatment contained 4–5 mice, and two random sections from each were quantified. Angiogenesis was quantified by direct count of vessels residing in the stroma interface and the matrigel implant, as previously described (Lee et al., 1999).

Results

Cyr61 is present in MSC cells and secretome

Initially, we utilized liquid chromatography tandem mass spectrometry (LC-MS/MS) technology to globally profile the proteome of Bone marrow-derived mesenchymal stem cells (MSCs). Two hundred and fifty eight (258) proteins were identified in MSC extracts with a stringent >95% confidence level (Supplemental Data 1). The sequence information of the identified peptides for each protein and the confidence levels of true proteomic identification are shown in Supplemental Data 2. The UniProt (http://beta.uniprot.org/) and Gene Ontology Tree Machine (http://bioinfo.vanderbilt.edu/gotm/) data bases were used for classification of subcellular localization and functional categorization of these identified proteins. As shown in Table 1, 54 proteins (20.93%) are categorized as secreted polypeptides. Among these identified polypeptides, some of them have been shown to

regulate various biological processes such as wound healing, inflammatory response, angiogenesis, cell proliferation, chemotaxis, and neurogenesis (Table 1).

Importantly, proteomic analysis showed that MSCs express Cyr61 polypeptides (Table 1 and Supplemental Data 1). Cyr61 polypeptides have been shown to regulate various biological activities (Leask and Abraham, 2006;Chen and Du, 2007). Thus, we focus on investigating the role of Cyr61 in mediating MSC-regulated physiological functions in the present study. The true identification of Cyr61 in MSCs was validated by immunostaining and immunoblotting technique (Fig. 1). Immunofluorescent microscopic analysis shows that Cyr61 polypeptides are abundantly expressed in MSCs (upper left part, Fig. 1A). In a control, there was no detectable signal when the immunostaining was performed in the absence of Cyr61 antibody (lower left part, Fig. 1A). The Nomarski micrographs corresponding to fluorescence images are shown in right parts of Figure 1A.

It has been shown that Cyr61 is a secreted polypeptide (Yang and Lau, 1991). Therefore, we examined whether Cyr61 polypeptides are present in the culture medium (secretome) of MSCs. The secretome was collected from MSCs cultured in plain DMEM medium for 24 h. To ensure that there was no intracellular proteins present in the secretome due to dead or lysed cells, MSCs were subjected to cell viability assay with Trypan blue exclusion method in a parallel control culture. More than 99% of cells were observed to exclude Trypan blue dye (data not shown), indicating that MSCs are viable in this culture condition. Moreover, the protein compositions of the secretome and cell extracts were further analyzed by SDS–PAGE. As shown in Supplemental Data 3, the protein profile of the secretome was markedly distinct from that of cell extracts. Together, these data suggest that the polypeptides present in MSC secretome are not resulted from cell death/lysis in the culture condition used to collect secretome. Next, MSC extracts and the collected secretome was subjected to immunoblotting analysis with anti-Cyr61 antibody to examine the presence of Cyr61 polypeptides. As shown in Figure 1B, Cyr61 polypeptides were detected in both MSC lysates as well as in secretome. These data together indicate that Cyr61 polypeptides are present in both cells and medium of MSC cultures.

Next, we examined whether Cyr61 polypeptides are expressed in freshly isolated MSCs, that is, the expression of Cyr61 in MSCs is not a culture artifact as a consequence of the in vitro cell culture. Thus, freshly isolated MSCs were subjected to immunostaining and immunoblotting analysis with Cyr61 antibody. As shown in Figure 2A,B, Cyr61 was clearly detected in freshly isolated MSCs. The fluorescence and immunoblot bands intensities of the freshly isolated cells were comparable to those of the cloned MSC cells, indicating that Cyr61 polypeptides are normally expressed by MSCs.

MSC secretome induces morphogenesis of endothelial cells in vitro

Cyr61 is a pro-angiogenic factor which induces morphogenesis of endothelial cells in vitro, and neovascularization in vivo (Obrien and Lau, 1992; Babic et al., 1998; Fataccioli et al., 2002). Thus, we investigated whether MSC secretome can induce morphogenesis of endothelial cells in vitro. HUVECs were cultured on three-dimensional matrigel in the presence or absence of various concentrations of MSC secretome. Plain Dulbecco minimal essential medium (DMEM) was used as a negative control. DMEM containing 10% (v/v) fetal bovine serum (FBS) or sphingosine-1-phosphate (S1P, 1 μM) was used as positive controls. As shown in Figure 3A,B, MSC secretome induces the formation of tubule-like structures of HUVECs in a dose-dependent manner. Moreover, the tubule induction obtained by treatment with secretome at a total protein concentration of 29 μg/ml was significantly greater than that obtained by treatment with 10% (v/v) FBS or S1P ($P < 0.01$, *t*-test).

Depletion of Cyr61 abrogates the angiogenesis-inducing capability of MSC secretome

To investigate whether the observed effect of MSC secretome in inducing angiogenesis is due to the Cyr61 polypeptides, we utilized the immunodepletion technique to remove Cyr61 polypeptides from MSC secretome. The secretome was incubated with beads cross-linked with anti-Cyr61 antibody, or with beads cross-linked with normal rabbit IgG as a negative control. After incubation, beads cross-liked with anti-Cyr61 or normal IgG were pelleted down by centrifugation. Then the secretome depleted with anti-Cyr61 or normal rabbit IgG were immunoblotted with anti-Cyr61 antibody. As shown in Figure 4A, Cyr61 polypeptides are effectively removed by incubating with anti-Cyr61 cross-linked beads (left lane), whereas beads cross-linked with normal IgG are unable to deplete Cyr61 from MSC secretome (middle lane). Subsequently, Cyr61-depleted secretome was used in endothelial morphogeneis assays in three-dimensional matrigel in vitro. As shown in Figure 4B,C, depletion of Cyr61 polypeptides completely abrogates the angiogenesis-inducing capability of MSC secretome. In contrast, the angiogenic response induced by secretome treated with beads cross-linked with normal IgG is comparable to that induced by the secretome without treatment.

Addition of recombinant Cyr61 polypeptides restores angiogenesis-inducing capability of Cyr61-depleted secretome

To further verify that Cyr61 plays a critical role in mediating angiogenesis-promoting activity of MSC secretome, we examined whether re-addition of purified Cyr61 is able to reinstate the angiogenic response of Cyr61-depleted secretome. Also, it has been well demonstrated that bone marrow-derived MSCs are mobilized to distal injury sites and are important in the wound-healing/injury-repairing process (Prockop, 1997; Annabi et al., 2003). We utilized human pulmonary arterial endothelial cells (HPAECs) for this depletion/replenishment assay, because HPAEC is a more physiologically relevant endothelial system than HUVECs in investigating the angiogenic response involved in the wound-healing/injury-repairing process. As shown in Figure 5A, Cyr61 was effectively removed after incubating with anti-Cyr61 cross-linked beads, whereas beads cross-linked with normal IgG were unable to deplete Cyr61 from MSC secretome. Cyr61-depleted secretome was reconstituted with human recombinant Cyr61 and used in tubule formation assays with HPAE cells in three-dimensional matrigel in vitro. Depletion of Cyr61 completely diminishes the angiogenic response, compared to the secretome treated with beads cross-linked with normal IgG and secretome without treatment (Fig. 5B,C). Importantly, re-addition of recombinant Cyr61 polypeptides completely restores the angiogenesis-promoting activity of Cyr61-depleted secretome. These data indicate that Cyr61 is an important factor contributing to the angiogenesis-inducing capability of mMSC secretome.

MSC secretome induces neovascularization in vivo

We next utilized the matrigel implant model in athymic mice to examine whether MSC secretome stimulates angiogenic response in vivo. Matrigel supplemented MSC secretome, Cyr61-depleted secretome reconstituted with or without recombinant Cyr61 was implanted subcutaneously in athymic mice, as we described previously (Passaniti et al., 1992; Lee et al., 1999). Matrigel supplemented with DMEM or S1P plus bFGF were used as negative and positive controls, respectively. As shown in Figure 6A, Matrigel supplemented with plain DMEM is unable to induce angiogenic response (left part, Fig. 6A), while the positive control, S1P-treated (middle part, Fig. 6A) and the secretome (right part, Fig. 6A) showed strong induction of neovascularization in the implanted matrigel (blue arrows, Fig. 6A). Histological examination of matrigels (Fig. 6B,C) supplemented with plain DMEM (upper left part, Fig. 6B) and secretome depleted of Cyr61 (upper right part, Fig. 6B) were unable to induce angiogenic response. In sharp contrast, the secretome (middle and lower left parts, Fig. 6B) and the Cyr61-depleted secretome reconstituted with recombinant Cyr61 (middle

and lower right parts, Fig. 6B) showed markedly induction of neovascularization in the stromal area (red arrows, middle right and left parts, Fig. 6B). Therefore, this data indicates that Cyr61 in MSC secretome is able to induce neovascularization in vivo.

Discussion

The participation of mesenchymal stem cells (MSCs) in tissue regeneration has been largely investigated according to the notion that these cells can themselves differentiate into different cell types, such as bone, cartilage, muscle, adipocytes, stroma, fibroblasts and endothelial cells (Prockop, 1997; Weissman, 2000; Phinney and Prockop, 2007). However, recent studies suggest that the ability of MSCs to alter the tissue microenvironment niche via secretion of factors may be important to tissue repair as their transdifferentiation capability (Chamberlain et al., 2007; Phinney and Prockop, 2007). For example, infusion of human MSCs into immunodeficient mice with acute myocardial infarction improves their cardiac function, although donor cells are not found 3 weeks after injection (Iso et al., 2007). Also, children with osteogenesis imperfecta who receive MSC treatment show significant improvement in growth velocity, bone mineral density, and ambulation; however, the population of MSC engrafted in tissues such as bone and skin is less than 1% (Horwitz et al., 2002). Therefore, elucidating the composition of the proteins secreted by MSCs would enhance our understanding of how these cells affect the environment niche, thus supporting tissue repair.

In a previous report (Sarojini et al., 2008), we attempted to use LC-MS/MS technology to profile the secretome of MSCs. In that report, only 19 secreted proteins were identified since straight (unconcentrated) cultural media were used directly for proteomic analysis. In the present study, we alternatively profiled the proteome of MSC extracts to identify other possible secreted proteins that are functionally important in regulating wound-healing response and that were not identified in our previous proteomic analysis of secretome. Two hundred and fifty eight cellular proteins were identified in MSCs, of which 54 (20.93%) are known to be secreted polypeptides (Table 1). Importantly, we observed that MSCs express Cyr61, a ~40-kDa protein member of the CCN family proteins. The presence of Cyr61 was confirmed by immunofluorescence staining and immunoblot analysis. In agreement, Phinney et al. also showed that Cyr61 polypeptides are expressed in human and murine MSCs (Phinney, 2007).

Cyr61 is a cysteine-rich, heparin binding protein encoded by an immediate early gene, and is known to be secreted into the extracellular milieu (Lau and Lam, 1999). Cyr61 was first reported to be secreted in fibroblasts, and is transcriptionally activated by the addition of serum and growth factors (e.g., basic fibroblast growth factor and transforming growth factor) (Lau and Lam, 1999). This protein is also expressed in all types of vascular cells, such as endothelial and smooth muscle cells (Lau and Lam, 1999; Grote et al., 2007), and is known to be transiently expressed in regenerating liver after partial hepatectomy (Lau and Lam, 1999). Cyr61 is associated with the extracellular matrix, and functionally capable of inducing angiogenic response by activating plasma membrane receptors of endothelial cells, and plays important roles in development and wound healing (Chen and Du, 2007). Moreover, Cyr61 is known to bind distinct integrins (e.g., $\alpha 6\beta 1$, $\alpha M\beta 2$, and $\alpha V\beta 3$), and regulate various biological activities such as cell adhesion, proliferation, migration, and neovascularization (Kireeva et al., 1998; Lau and Lam, 1999; Chen et al., 2000; Schober et al., 2002). Furthermore, Cyr61 knockout mice exhibit vascular defects during embryogenesis and fetal development, suggesting that Cyr61 plays a critical role in regulating the development and maintenance of vasculature (Mo et al., 2002).

In this study, Cyr61 was shown to be present in the secretome of murine mesenchymal stem cells by immunoblot analysis (Fig. 1B). Consistent with our observation, Sze et al. previously detected Cyr61 in hESC-derived MSC secretome (Sze et al., 2007). Together, it suggests that Cyr61 secreted by MSCs may have an autocrine or paracrine function in regulating biological responses mediated by MSCs. By using in vitro and in vivo angiogenic assays, we showed that the secretome of MSCs promotes morphogenesis of endothelial cells in a dose-dependent manner in vitro, as well as neovascularization in vivo. In addition, immunodepletion of Cyr61 abrogates the angiogenesis-promoting capability of MSC secretome in vitro and in vivo. Importantly, addition of human recombinant Cyr61 to the depleted secretome restores its angiogenic activity. These data collectively demonstrate that Cyr61 is an important factor in the secretome of mMSCs that contributes to the promotion of angiogenesis. It is worthy to be noted that mesenchymal stem cells have been previously shown to be capable of inducing angiogenic response (Phinney, 2007;Wu et al., 2007). Moreover, a number of angiogenic factors have been identified in cell and secretome of MSCs (Phinney, 2007;Sze et al., 2007;Wu et al., 2007). In the present study, we provide evidence directly demonstrating that Cyr61 polypeptides contribute to the angiogenesis-promoting capability of MSCs. However, other MSC secreted factors which are not tested in this work may also synergistically contribute to angiogenic properties of MSC secretome.

Previously, we showed that MSC secretome induces chemotactic response of human fibroblast cells (Sarojini et al., 2008). Moreover, we demonstrated that pigment epithelium-derived factor (PEDF) is a critical fibroblast chemoattractant present in the MSC secretome. Collectively, these data suggest that MSCs secrete a panel of functionally active factors that can remodel or regulate the tissue microenvironment niche, cumulatively ensuring successful wound healing and injury repair. The understanding of functions of the MSC-secreted molecules and how they regulate the tissue microenvironment niche may allow the development of therapeutic strategies to enhance the recruitment of resident cells to repair injured or damaged tissues. Factors such as PEDF secreted by MSCs may stimulate migration of fibroblasts needed for scaffold building, while the secretion of Cyr61 promotes neovascularization.

Supplementary Material

Refer to Web version on PubMed Central for supplementary material.

Acknowledgments

The authors acknowledge proof-reading and helpful suggestions of Mr. Alan N. Bloch during the preparation of this manuscript. We thank Dr. Jaiwei Zhao for immunoblotting analysis, and Derek Terry for assistance with experiments involving the use of animals. This work was supported by a grant from the Defense Advance Research Project Agency (DARPA) of the U.S. Department of Defense to E. W.

Contract grant sponsor: Defense Advance Research Project Agency;

Contract grant number: W911NF-06-1-0161.

Literature Cited

Annabi B, Lee YT, Turcotte S, Naud E, Desrosiers RR, Champagne M, Eliopoulos N, Galipeau J, Beliveau R. Hypoxia promotes murine bone-marrow-derived stromal cell migration and tube formation. Stem Cells 2003;21:337–347. [PubMed: 12743328]

Babic AM, Kireeva ML, Kolesnikova TV, Lau LF. CYR61, a product of a growth factor-inducible immediate early gene, promotes angiogenesis and tumor growth. Proc Natl Acad Sci USA 1998;95:6355–6360. [PubMed: 9600969]

Chamberlain G, Fox J, Ashton B, Middleton J. Concise review: Mesenchymal stem cells: Their phenotype, differentiation capacity, immunological features, and potential for homing. Stem Cells 2007;25:2739–2749. [PubMed: 17656645]

Chen Y, Du XY. Functional properties and intracellular signaling of CCN1/Cyr61. J Cell Biochem 2007;100:1337–1345. [PubMed: 17171641]

Chen NY, Chen CC, Lau LF. Adhesion of human skin fibroblasts to Cyr61 is mediated through integrin alpha(6)beta(1) and cell surface heparan sulfate proteoglycans. J Biol Chem 2000;275:24953–24961. [PubMed: 10821835]

Cong Y-S, Fan E, Wang E. Simultaneous proteomic profiling of four different growth states of human fibroblasts, using amine-reactive isobaric tagging reagents and tandem mass spectrometry. Mech Ageing Dev 2006;127:332–343. [PubMed: 16434083]

Fataccioli V, Abergel V, Wingertsmann L, Neuville P, Spitz E, Adnot S, Calenda V, Teiger E. Stimulation of angiogenesis by Cyr61 gene: A new therapeutic candidate. Hum Gene Ther 2002;13:1461–1470. [PubMed: 12215267]

Grote K, Salguero G, Ballmaier M, Dangers M, Drexler H, Schieffer B. The angiogenic factor CCN1 promotes adhesion and migration of circulating CD34(+) progenitor cells: Potential role in angiogenesis and endothelial regeneration. Blood 2007;110:877–885. [PubMed: 17429007]

Hla T, Maciag T. An abundant transcript induced in differentiating human endothelial-cells encodes a polypeptide with structural similarities to G-protein-coupled receptors. J Biol Chem 1990;265:9308–9313. [PubMed: 2160972]

Horwitz EM, Gordon PL, Koo WKK, Marx JC, Neel MD, McNall RY, Muul L, Hofmann T. Isolated allogeneic bone marrow-derived mesenchymal cells engraft and stimulate growth in children with osteogenesis imperfecta: Implications for cell therapy of bone. Proc Natl Acad Sci USA 2002;99:8932–8937. [PubMed: 12084934]

Iso Y, Spees JL, Serrano C, Bakondi B, Pochampally R, Song YH, Sobel BE, Delafontaine P, Prockop DJ. Multipotent human stromal cells improve cardiac function after myocardial infarction in mice without long-term engraftment. Biochem Biophys Res Commun 2007;354:700–706. [PubMed: 17257581]

Kireeva ML, Lam SCT, Lau LF. Adhesion of human umbilical vein endothelial cells to the immediate-early gene product Cyr61 is mediated through integrin alpha(v)beta(3). J Biol Chem 1998;273:3090–3096. [PubMed: 9446626]

Lau LF, Lam SCT. The CCN family of angiogenic regulators: The integrin connection. Exp Cell Res 1999;248:44–57. [PubMed: 10094812]

Leask A, Abraham DJ. All in the CCN family: Essential matricellular signaling modulators emerge from the bunker. J Cell Sci 2006;119:4803–4810. [PubMed: 17130294]

Lee MJ, Evans M, Hla T. The inducible G protein-coupled receptor edg-1 signals via the G(i)/nitrogen-activated protein kinase pathway. J Biol Chem 1996;271:11272–11279. [PubMed: 8626678]

Lee MJ, Thangada S, Claffey KP, Ancellin N, Liu CH, Kluk M, Volpi M, Sha'afi RI, Hla T. Vascular endothelial cell adherens junction assembly and morphogenesis induced by sphingosine-1-phosphate. Cell 1999;99:301–312. [PubMed: 10555146]

Mo FE, Muntean AG, Chen CC, Stolz DB, Watkins SC, Lau LF. CYR61 (CCN1) is essential for placental development and vascular integrity. Mol Cell Biol 2002;22:8709–8720. [PubMed: 12446788]

Obrien TP, Lau LF. Expression of the growth factor-inducible immediate early gene Cyr61 correlates with chondrogenesis during mouse embryonic-development. Cell Growth Differ 1992;3:645–654. [PubMed: 1419914]

Passaniti A, Taylor RM, Pili R, Guo Y, Long PV, Haney JA, Pauly RR, Grant DS, Martin GR. Methods in laboratory investigation—A simple, quantitative method for assessing angiogenesis and antiangiogenic agents using reconstituted basement-membrane, heparin, and fibroblast growth-factor. Lab Invest 1992;67:519–528. [PubMed: 1279270]

Phinney DG. Biochemical heterogeneity of mesenchymal stem cell populations—Clues to their therapeutic efficacy. Cell Cycle 2007;6:2884–2889. [PubMed: 18000405]

Phinney DG, Prockop DJ. Concise review: Mesenchymal stem/multipotent stromal cells: The state of transdifferentiation and modes of tissue repair—Current views. Stem Cells 2007;25:2896–2902. [PubMed: 17901396]

Prockop DJ. Marrow stromal cells as stem cells for nonhematopoietic tissues. Science 1997;276:71–74. [PubMed: 9082988]

Reyes M, Dudek A, Jahagirdar B, Koodie L, Marker PH, Verfaillie CM. Origin of endothelian progenitors in human postnatal bone marrow. J Clin Invest 2002;109:337–346. [PubMed: 11827993]

Sarojini H, Estrada R, Lu HW, Dekova S, Lee MJ, Gray RD, Wang E. PEDF from mouse mesenchymal stem cell secretome attracts fibroblasts. J Cell Biochem 2008;104:1793–1802. [PubMed: 18348263]

Schober JM, Chen NY, Grzeszkiewicz TM, Jovanovic I, Emeson EE, Ugarova TP, Ye RD, Lau LF, Lam SCT. Identification of integrin alpha(M)beta(2) as an adhesion receptor on peripheral blood monocytes for Cyr61 (CCN1) and connective tissue growth factor (CCN2): Immediate-early gene products expressed in atherosclerotic lesions. Blood 2002;99:4457–4465. [PubMed: 12036876]

Sze SK, de Kleijn DPV, Lai RC, Tan EKW, Zhao H, Yeo KS, Low TY, Lian Q, Lee CN, Mitchell W, El Oakley RM, Lim SK. Elucidating the secretion proteome of human embryonic stem cell-derived mesenchymal stem cells. Mol Cell Proteomics 2007;6:1680–1689. [PubMed: 17565974]

Tomanek RJ, Schatteman GC. Angiogenesis: New insights and therapeutic potential. Anat Rec 2000;261:126–135. [PubMed: 10867630]

Weissman IL. Translating stem and progenitor cell biology to the clinic: Barriers and opportunities. Science 2000;287:1442–1446. [PubMed: 10688785]

Wu YJ, Chen L, Scott PG, Tredget EE. Mesenchymal stem cells enhance wound healing through differentiation and angiogenesis. Stem Cells 2007;25:2648–2659. [PubMed: 17615264]

Yang GP, Lau LF. Cyr61, product of a growth factor-inducible immediate early gene, is associated with the extracellular-matrix and the cell-surface. Cell Growth Differ 1991;2:351–357. [PubMed: 1782153]

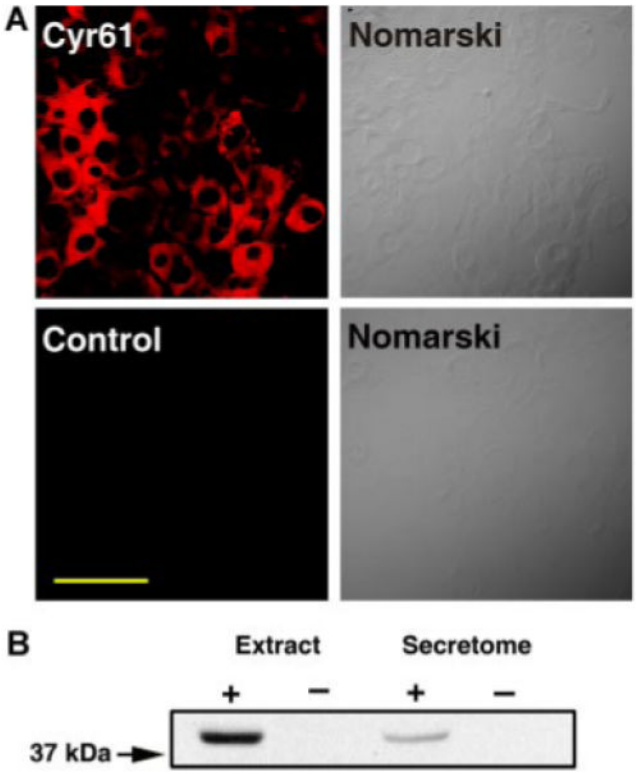

Fig. 1.

The expression of Cyr61 in MSCs. A: mMSCs were immunostained with (upper left part) or without (lower left part) anti-Cyr61 antibody, as described in Experimental Procedures Section. The corresponding Nomarski micrographs are shown in the right parts. Scale bar, 100 μm. B: Western blot analysis of mMSC cellular extracts and secretome with Cyr61 antibody. Left lane, cellular extracts (66 μg); second lane, extraction buffer (negative control); third lane, secretome (66 μg); right lane, plain-DMEM (negative control). Note that Cyr61 polypeptides are detected in both cell extracts and secretome. [Color figure can be viewed in the online issue, which is available at www.interscience.wiley.com.]

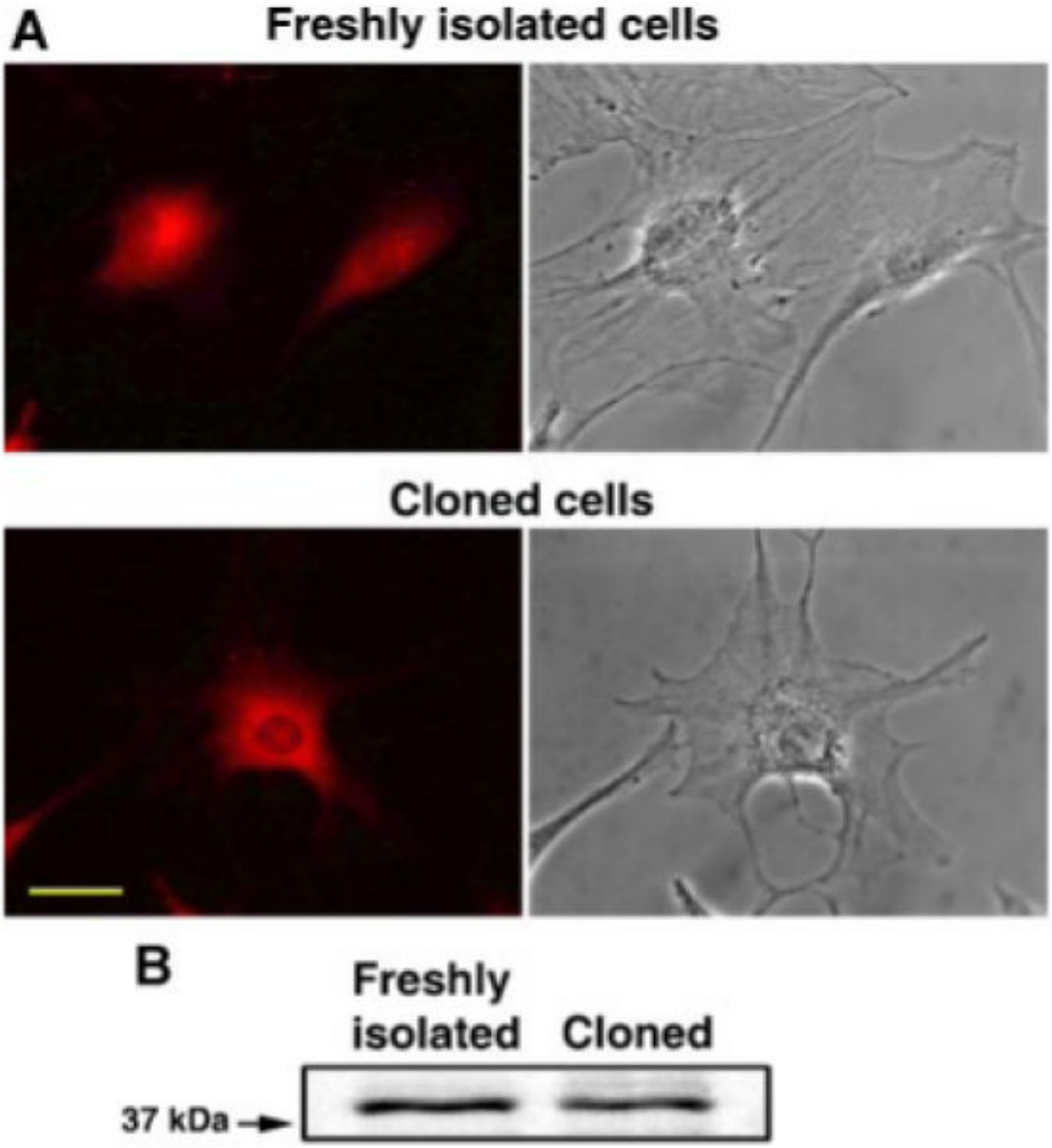

Fig. 2.

The expression of Cyr61 in freshly isolated and cloned MSCs. A: Freshly isolated (upper left part) and cloned (lower left part) MSCs were immunostained with anti-Cyr61 antibody, as described in Experimental Procedures Section. The corresponding phase contrast micrographs are shown in the upper and lower right parts, respectively. Scale bar 40 μm. B: Western blot analysis of freshly isolated and cloned MSCs with Cyr61 antibody. Note that Cyr61 polypeptides are detected in both freshly isolated and cloned MSC cells. [Color figure can be viewed in the online issue, which is available at www.interscience.wiley.com.]

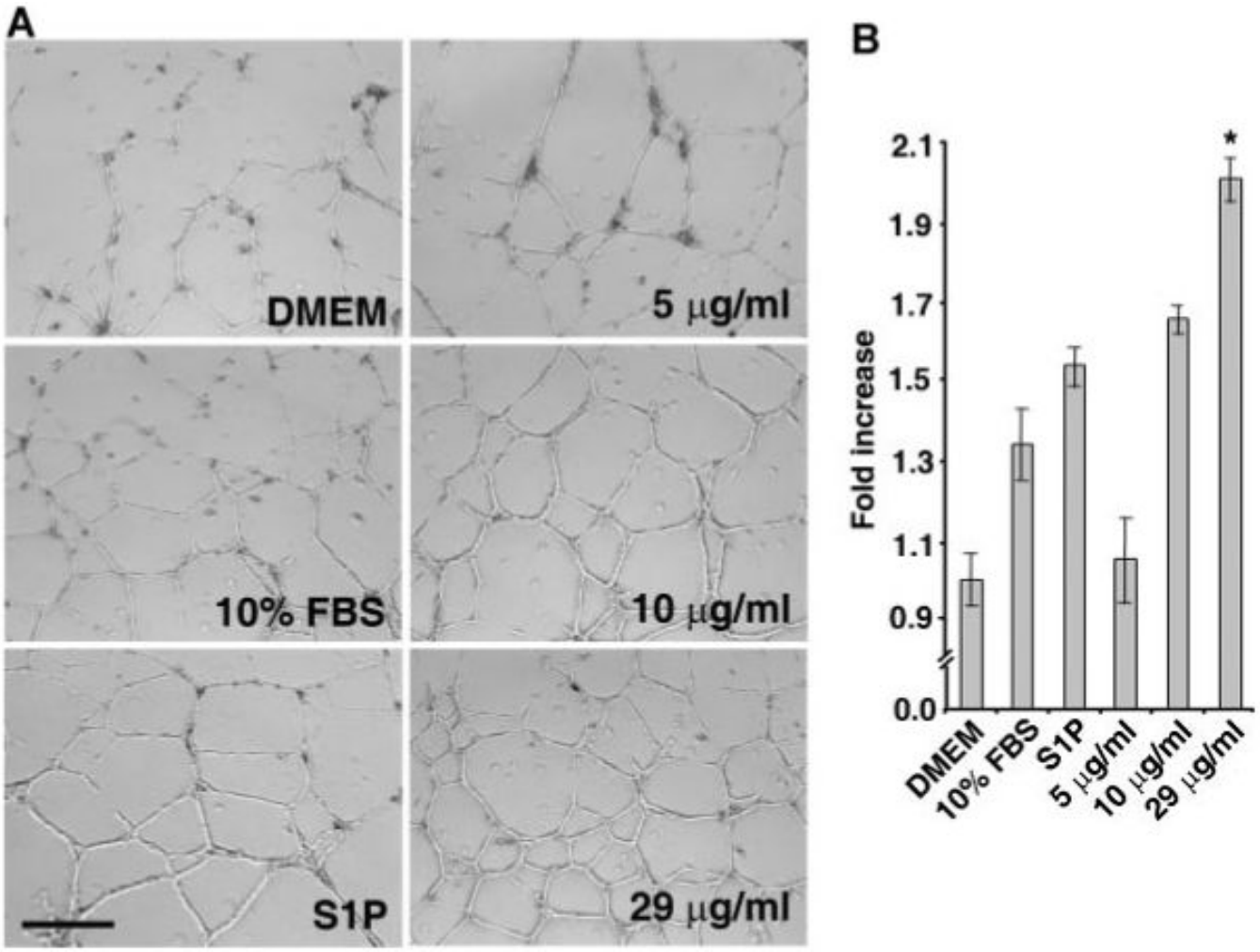

Fig. 3.

MSC secretome promotes morphogenesis of endothelial cells in vitro. A: HUVECs were plated on three-dimensional matrigel in the presence or absence of indicated concentrations of MSC secretome. Plain DMEM medium was used as a negative control, 10% (v/v) FBS in DMEM and S1P (1 μM) were used as positive controls. B: Quantitative analysis of tubule length. Note that MSC secretome dose-dependently stimulates morphogenic response of endothelial cells. Also note that the formation of tubule-like structures induced by MSC secretome at total protein concentration of 29μg/ml is significantly greater than that induced by 10% FBS and S1P (*$P < 0.01$, *t*-test). The quantification of total tube length was done by addition of the tubule length from five random fields per well. Data are Mean ± SD from three wells. Scale bar, 400 μm.

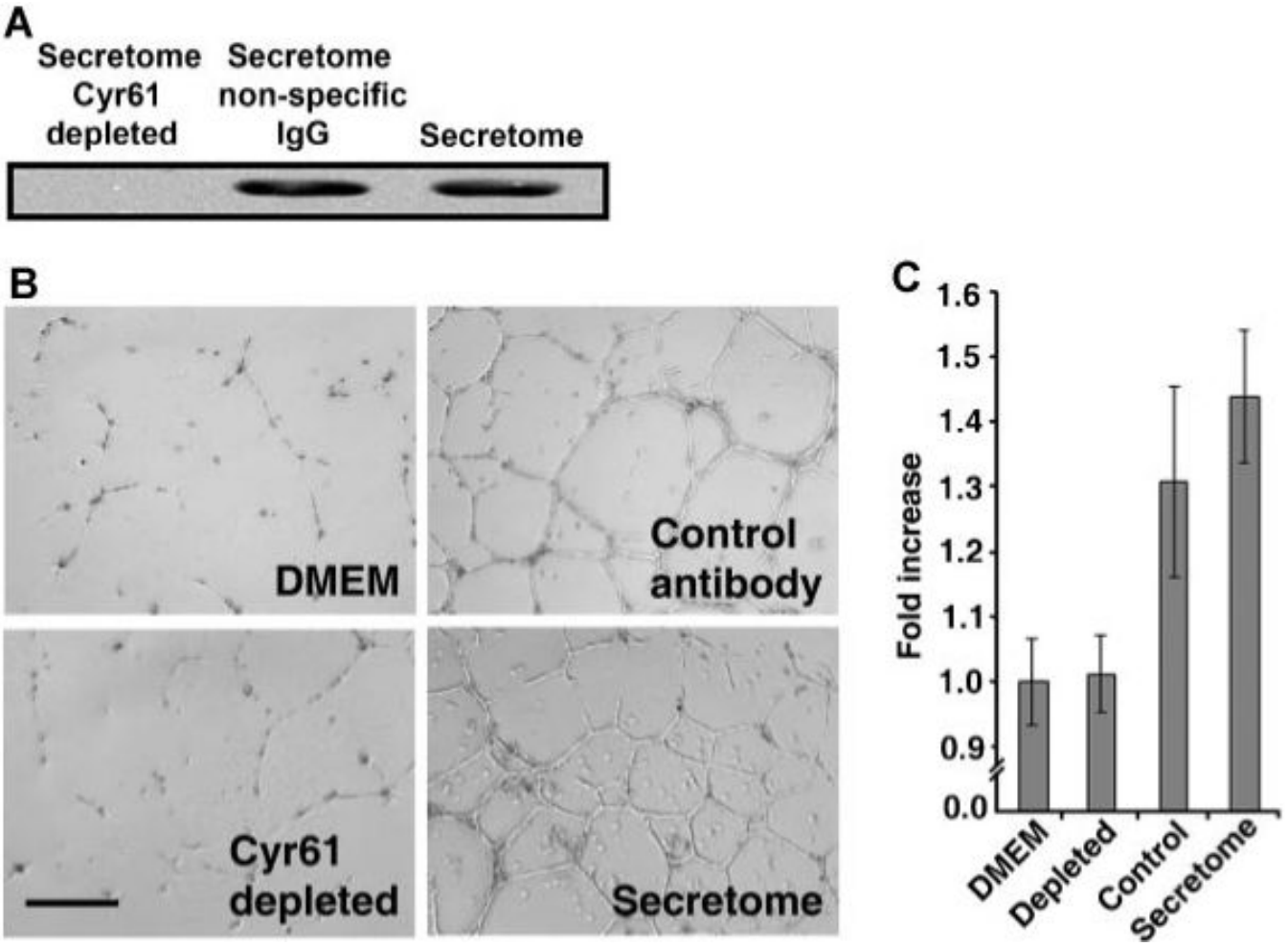

Fig. 4.

Depletion of Cyr61 abrogates angiogenic response of MSC secretome. Protein A/G beads were cross-linked with anti-Cyr61 or normal rabbit IgG, as described (Lee et al., 1996). MSC secretome was then incubated with antibody cross-linked beads, as described in Experimental Procedures Section. A: The secretomes treated with anti-Cyr61 or normal IgG were immunoblotted with anti-Cyr61. Right lane, secretome without Protein A/G beads treatment. Sixty-six microgram proteins were loaded in each lane. B: Morphogenesis of HUVECs in three-dimensional matrigel induced by secretome and secretome depleted with anti-Cyr61 or normal IgG. C: Quantitative analysis of tubule length. Note that depletion of Cyr61 from MSC secretome completely abolishes the angiogenesis-inducing capability of MSC secretome. Control, secretome treated with beads cross-linked with normal rabbit IgG. The total tubule length quantification was done by addition of the tubule length from five random fields per well. Data are Mean ± SD of triplicate determinations. Scale bar, 400 μm.

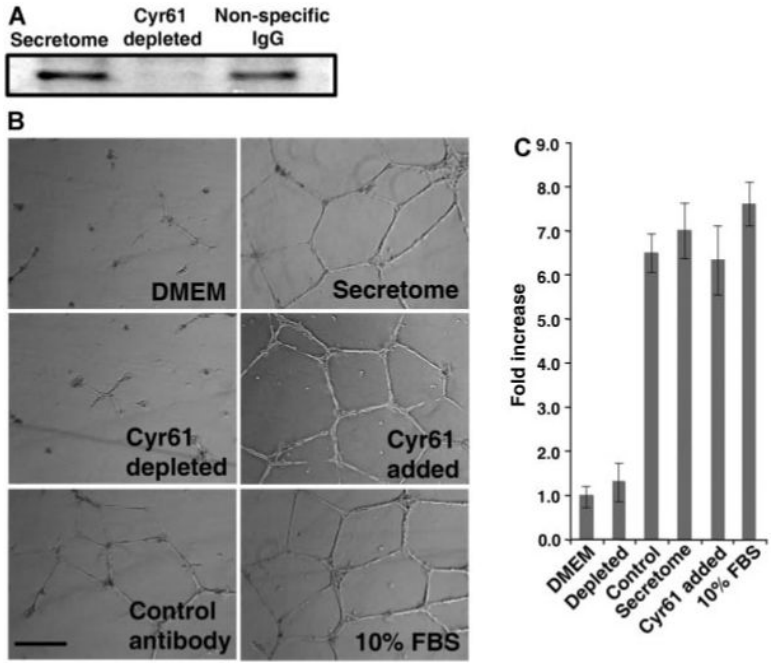

Fig. 5.

Addition of Cyr61 restores the angiogenic activity of Cyr61-depleted MSC secretome. Immunodepletion was performed as described in Figure 4 and Experimental Procedures Section. A: After incubation, the secretomes were immunoblotted with anti-Cyr61. In all cases, 66 μg proteins per well were loaded. B: Morphogenesis of HPAE cells in matrigel induced by secretome, secretome depleted with anti-Cyr61 or normal IgG, and Cyr61-depleted secretome supplemented with 0.1 μg/ml human recombinant Cyr61 polypeptides (Cell Sciences). DMEM and 10% (v/v) FBS were used as negative and positive controls, respectively. C: Quantitative analysis of tubule length. Note that depletion of Cyr61 from MSC secretome completely abrogates the angiogenesis-inducing capability of MSC secretome. Also note that the addition of recombinant human Cyr61 restores the angiogenesis-promoting activity of the Cyr61-depleted secretome. The total tubule length quantification was done by addition of the tubule length from five random fields per well. Data are Mean ± SD of triplicate determinations. Scale bar, 400 μm.

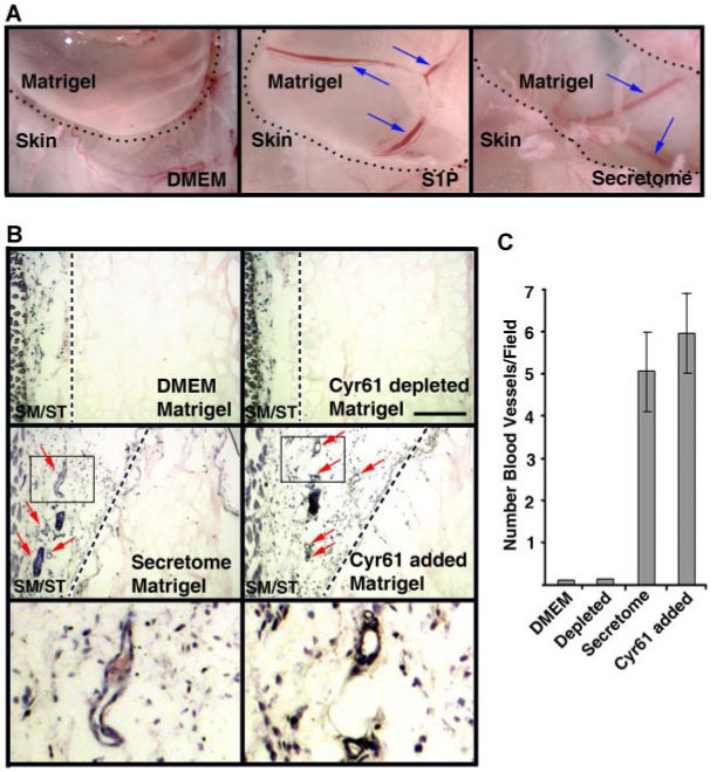

Fig. 6.

MSC secretome promotes neovascularization in vivo. A: Low-power micrographs of angiogenic responses in implanted matrigel supplemented with Dulbecco minimal essential medium (DMEM, negative control), sphingosine-1-phosphate (S1P) + FGF-2 + heparin (positive control), and MSC secretome. Note that S1P and secretome markedly promotes neovascularization in the implanted matrigel plugs(blue arrows). In contrast, there is no neovessels in the matrigel plug supplemented with DMEM. The dotted lines demarcate the implanted matrigel plugs. B: Histological analysis of hematoxylin/eosin stained sections of matrigel supplemented with DMEM, MSC secretome, Cyr61-depleted secretome in the presence or absence of recombinant Cy61 polypeptides. The lower parts are high-power views of the boxed areas indicated in the middle parts. Note that the secretome and Cyr61-depleted secretome reconstituted with recombinant Cyr61 enhance the formation of neovasculatures in the stromal area (red arrows). SM, skeletal muscle; and ST, stroma. Scale bars, 200 μm. C: Quantification of neovessels. Angiogenesis in matrigel plugs was quantified by direct counting the vasculature structures from five stained sections. Data are mean ± SD from triplicate determinations. [Color figure can be viewed in the online issue, which is available at www.interscience.wiley.com.]

TABLE 1

Secreted mMSC proteins determined by the UniProt and gene ontology tree machine data bases

N	SwissProt accession #	Name
1	P09103	Protein disulfide-isomerase precursor
2	P27773	Protein disulfide-isomerase A3 precursor
3	P35441	Thrombospondin-1 precursor
4	P11276	Fibronectin precursor
5	P14211	Calreticulin precursor
6	P11087	Collagen alpha-1(I) chain precursor
7	P07356	Annexin A2
8	P16110	Galectin-3
9	P19324	47 kDa heat shock protein precursor
10	Q07235	Glia-derived nexin precursor
11	Q61838	Alpha-2-macroglobulin precursor
12	P01029	Complement C4-B precursor
13	P16045	Galectin-1
14	O08795	Glucosidase 2 subunit beta precursor
15	P08113	Endoplasmin precursor
16	O08807	Peroxiredoxin-4
17	P24369	Peptidyl-prolyl cis-trans isomerase B precursor
18	Q9Z0J0	Epididymal secretory protein E1 precursor
19	P63158	High mobility group protein B1
20	Q60715	Prolyl 4-hydroxylase subunit alpha-1 precursor
21	Q9D0K2	Succinyl-CoA:3-ketoacid-coenzyme A transferase 1
22	P05202	Aspartate aminotransferase, mitochondrial precursor
23	Q9R0B9	Procollagen-lysine, 2-oxoglutarate 5-dioxygenase 2 precursor
24	Q03265	ATP synthase subunit alpha, mitochondrial precursor
25	Q60847	Collagen alpha-1(XII) chain precursor
26	Q9QXT0	Protein canopy homolog 2 precursor
27	Q9ERE7	Mesoderm development candidate 2
28	Q01149	Collagen alpha-2(I) chain precursor
29	P37889	Fibulin-2 precursor
30	P55302	Alpha-2-macroglobulin receptor-associated protein precursor
31	P70180	Atrial natriuretic peptide clearance receptor precursor
32	Q64191	N(4)-(beta-N-acetylglucosaminyl)-L-asparaginase precursor
33	P07214	SPARC precursor
34	Q61704	Inter-alpha-trypsin inhibitor heavy chain H3 precursor
35	Q99M71	Mammalian ependymin-related protein 1 precursor
36	P35486	Pyruvate dehydrogenase E1 component alpha subunit
37	Q9JKR6	Hypoxia up-regulated protein 1 precursor

N	SwissProt accession #	Name
38	P63028	Translationally controlled tumor protein
39	P28653	Biglycan precursor
40	O54998	FK506-binding protein 7 precursor
41	Q9D1Q6	Thioredoxin domain-containing protein 4 precursor
42	Q91W10	Zinc transporter ZIP8
43	P13020	Gelsolin precursor
44	Q9D172	ES1 protein homolog, mitochondrial precursor
45	Q61207	Sulfated glycoprotein 1 precursor
46	P50543	Protein S100-A11
47	Q9Z247	FK506-binding protein 9 precursor
48	Q3TCN2	Putative phospholipase B-like 2 precursor
49	P57759	Endoplasmic reticulum protein ERp29 precursor
50	P34884	Macrophage migration inhibitory factor
51	P29268	Connective tissue growth factor precursor
52	O55126	Protein NipSnap homolog 2
53	P18406	Cysteine-rich, angiogenic inducer, 61 (Cyr61)
54	P35564	Calnexin precursor

Proteins are ordered from the highest confident level (>99%) to the lowest confident level (≥95%) by using the ProteinPilot software v.2.0.1 software (Applied Biosystems, Inc.).